THE JOURNAL OF PHYSICAL CHEMISTRY A

 VOLUME 107, NUMBER 23, JUNE 12, 2003

LETTERS

Hyperthermal Reactions of O(^{3}P) with Alkanes: Observations of Novel Reaction Pathways in Crossed-Beams and Theoretical Studies

Donna J. Garton and Timothy K. Minton*

Department of Chemistry and Biochemistry, Montana State University, Bozeman, Montana 59717

Diego Troya, Ronald Pascual, and George C. Schatz*

Department of Chemistry, Northwestern University, Evanston, Illinois 60208-3133

Received: December 16, 2002; In Final Form: February 24, 2003

The reactions of O(^{3}P) with CH_4, CH_3CH_3, and $CH_3CH_2CH_3$ at center-of-mass collision energies in the range of 2.8−3.9 eV have been investigated with crossed-beams experiments and with direct dynamics calculations. The experiments and calculations both provide evidence for previously unobserved reaction pathways which principally lead to O-atom addition and subsequent H-atom elimination or C−C bond breakage: O(^{3}P) + RH → RO + H or R′O + R″. In addition, the expected H-atom abstraction reaction to form OH has been observed. The H-atom abstraction reactions have modest barriers in the range ∼0.1−0.3 eV, whereas the addition pathways have barriers greater than ∼1.8 eV. Nevertheless, theory predicts that abstraction and addition reactions occur with similar probabilities at the collision energies of these studies. Although high barriers prevent the addition reactions from occurring in most thermal environments, such reactions might be important in low-Earth orbit, where spacecraft surfaces and exhaust gases suffer high-energy collisions with ambient atomic oxygen.

I. Introduction

Spacecraft in low-Earth orbit (LEO) collide with ambient oxygen atoms (assumed to be in the ground O(^{3}P) state) at high relative velocities (∼8 km s^{-1}).[1] These hyperthermal collisions result in erosion of hydrocarbon polymer surfaces[2] and in chemiluminescent emissions from thruster exhaust streams.[1] This regime of collision energies allows high reaction barriers to be surmounted; therefore, the gas−surface and gas-phase reactions of O(^{3}P) even with relatively simple (saturated) hydrocarbons may involve many more reaction pathways than the well-studied H-atom abstraction reaction.[3] Although there have been numerous studies of the dynamics of the reactions of low energy O(^{1}D) with small alkanes,[4−6] experimental and theoretical studies of the corresponding gas-phase dynamics of hyperthermal O(^{3}P) reactions do not exist. However, a recent theoretical calculation has been performed on the transition state structures and energies for C−C bond breaking channels in the reaction of O(^{3}P) with small alkanes.[7] For the O(^{3}P) + CH_3CH_3 reaction to form CH_3O + CH_3, the barrier to reaction was found to be approximately 2 eV. This theoretical result suggests that a variety of exotic reaction pathways might become accessible at the high collision energies that exist between ambient O atoms and a spacecraft in LEO. In addition, the opening of additional reaction pathways might explain why the degradation of hydrocarbon-based polymers by hyperthermal (5 eV) O atoms appears to be much more important than that of lower energy O atoms.[2]

* To whom correspondence should be addressed. (T.K.M.) Phone: (406) 994-5394. Fax: (406) 994-6011. E-mail: tminton@montana.edu. (G.C.S.) Phone: (847) 491-5657. Fax: (847) 491-7713. E-mail: schatz@chem.northwestern.edu.

10.1021/jp0226026 CCC: $25.00
Published on Web 05/15/2003

Experimental studies of $O(^3P)$-atom reactions with saturated hydrocarbon surfaces have revealed much about the gas−surface interaction dynamics, but they have not verified the suggested direct attack on a carbon atom. Many experiments have investigated surface oxidation resulting from O-atom bombardment of hydrocarbon polymers, whereas others have probed the volatile species that are ejected from the surface.[2] CO and CO_2 are believed to be important volatile species that carry mass away from the surface during steady-state bombardment by O atoms,[8] but the importance of other volatile carbon-containing species is currently unknown. Initial interactions/reactions have been shown to involve atom−surface energy transfer and H-atom abstraction to form OH.[9] The dynamical behavior of the OH product indicates a gas-phase-like process where the incident hyperthermal oxygen atom is viewed as interacting with a localized region of the surface. This result suggests that a detailed study of model gas-phase reactions at hyperthermal collision energies will be representative of both gas-phase and gas−surface reactions between $O(^3P)$ and spacecraft in LEO.

We have undertaken a detailed investigation of the model reactions of $O(^3P)$ with small hydrocarbon molecules, CH_4, CH_3-CH_3, and $CH_3CH_2CH_3$, at collision energies comparable to those encountered in LEO. This letter, which combines the results of crossed-beams experiments and direct dynamics calculations, reports the first identification of the reaction pathways in these model hyperthermal-atomic-oxygen reactions.

II. Experimental Details

The experiments employed a crossed molecular beams apparatus[9,10] equipped with a laser detonation source[11] that produces a pulsed hyperthermal beam containing atomic oxygen in its ground electronic state, $O(^3P)$.[12] This O-atom beam was crossed at right angles by a pulsed supersonic alkane beam. A synchronized chopper wheel was used to select a narrow portion of the hyperthermal beam pulse. The average (laboratory) translational energy of the hyperthermal O atoms was 5.4 eV, and the energy spread (fwhm) was ∼1 eV. The fraction of O atoms in the hyperthermal beam was ∼70%. The only other component in the beam was molecular oxygen, which had an average translational energy and width roughly double those of the atomic component. The supersonic alkane beams had nominal velocities of 800, 990, and 1100 m s^{-1} for propane, ethane, and methane, respectively. Center-of-mass (c.m.) collision energies were 3.9 eV (O + $CH_3CH_2CH_3$), 3.5 eV (O + CH_3CH_3), and 2.8 eV (O + CH_4). Reaction products and elastically (or inelastically) scattered products were monitored with a mass spectrometer detector, which can rotate about the crossing point of the two beams. The number density distributions of products scattered from the crossing region of the two beams were collected as a function of their arrival time in the electron-bombardment ionizer of the detector. These time-of-flight (TOF) distributions were collected at a variety of detection, or laboratory, angles. (The O-atom beam direction is taken to be a laboratory angle of zero, and the positive angular direction is defined by a rotation from the O-atom beam toward the alkane beam.) Center-of-mass velocity flux maps have not yet been generated, as the distribution of relative velocities (collision energies) provides poor velocity resolution. The focus of the current experiments is thus on the identification of the reaction pathways.

III. Computational Details

The $O(^3P)$-atom reactions with the three alkanes were investigated with the quasiclassical trajectory method where the energy gradients are computed as the trajectory is evolved ("on the fly") with the use of different levels of electronic structure theory. Density functional calculations (B3LYP/6-31G*)[13] were used for the highest level of theory, but the tremendous computational expense involved when using this method limited our total number of trajectories to around 300 for each of the three systems considered. More extensive calculations (about 10 000 trajectories per system) were carried out with the use of the MSINDO semiempirical Hamiltonian,[14] which furnishes reaction energies and barriers noticeably closer to density functional calculations than do those obtained with standard semiempirical Hamiltonians such as PM3 or AM1. The close agreement between MSINDO and B3LYP/6-31G* results that we find establishes the legitimacy of the semiempirical calculations, and the reduced computational cost allows us to analyze detailed aspects of the microscopic reaction mechanisms with reasonable accuracy.

IV. Experimental Results

The reaction, $O(^3P) + CH_3CH_2CH_3$, exhibits basic pathways that are analogous to the reactions of $O(^3P)$ with CH_4 and CH_3-CH_3 (although the reaction with CH_4 does not have the possibility for C−C bond breakage). As the reaction with propane serves to illustrate all of the different types of reaction mechanisms that have been observed for the hyperthermal reactions of $O(^3P)$ with these small alkanes, only the details of the results for the propane reaction are presented here.[15]

Time-of-flight (TOF) distributions were collected at lab angles from −30° to +50° following the interaction of the O-atom and propane beams. Representative TOF distributions, collected at a lab angle of 10° for m/z = 16, 17, 29, 30, and 31, are shown in Figure 1. Weak signals (not shown) were also observed for m/z = 43 ($C_2H_3O^+$), 56 ($C_3H_4O^+$), and 57 ($C_3H_5O^+$). Although the TOF distributions indicate a propensity for nonreactive scattering (note the large signal at m/z = 16), there is also significant reactive scattering to produce the OH radical (m/z = 17) and other oxygen-containing hydrocarbon species (detected at ionizer fragments m/z = 29, 30, 31, 43, 56, and 57).

The structure in the TOF distributions collected at m/z = 29 and 30 suggests the occurrence of multiple reaction pathways. Signals at m/z = 29, 30, and 31 may arise from formation (and ionizer fragmentation) of C_2H_5 (m/z = 29 only), CH_3O, C_2H_5O, C_3H_7O, or C_3H_6O (propanone or propanal). The long flight time of the m/z = 31 signal (peak near 140 μs) suggests that its origin lies in the same product that gives rise to the slow peaks in the m/z = 29 and 30 TOF distributions. Of the C_3 products, C_3H_7O is considered to be most likely (*vide infra*). The C_3H_7O (and perhaps C_3H_6O) product is undoubtedly responsible for the weak signals observed at m/z = 56 and 57. Figure 2 shows TOF distributions for m/z = 29 at three different lab angles. Lines drawn on the distributions indicate the minimum possible flight times at which CH_3O/C_2H_5, C_2H_5O, and C_3H_7O/C_3H_6O products are expected to arrive at the detector, given the nominal c.m. collision energy of 3.9 eV. (Note that CH_3O/C_2H_5 and C_3H_7O/C_3H_6O indicate pairs of potential products that can be detected at m/z = 29 and that should have similar velocities, within each pair, because the products in each pair have similar masses and will thus have similar arrival times if the release to product translation is similar.) In reality, there is a spread in the TOF distributions resulting from the time width of the O-atom beam pulse. This spread may lead to detected signals at times shorter than the position of each line by approximately 16 μs. The very slow signal, with flight times longer than ∼125 μs, is believed

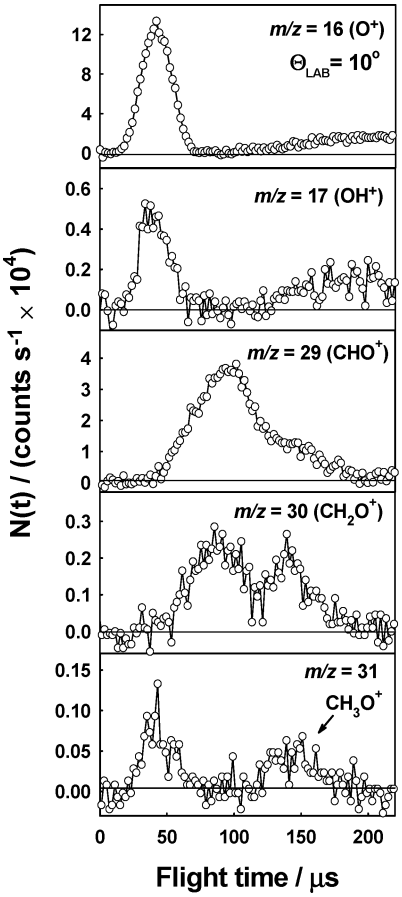

Figure 1. TOF distributions of products detected at $m/z = 16$, 17, 29, 30, and 31 from the reaction, $O(^3P) + C_3H_8$, collected with a detector angle of 10° with respect to the O-atom beam. Broad signals at long flight times in the $m/z = 16$ and 17 TOF distributions arise from slow transport of gases from the beam source chambers into the detector. The peak at short times in the $m/z = 31$ TOF distribution comes from mass leakage of elastically scattered O_2, whereas the peak near 140 μs arises from ionizer fragmentation of the C_3H_7O (or possibly C_3H_6O) product.

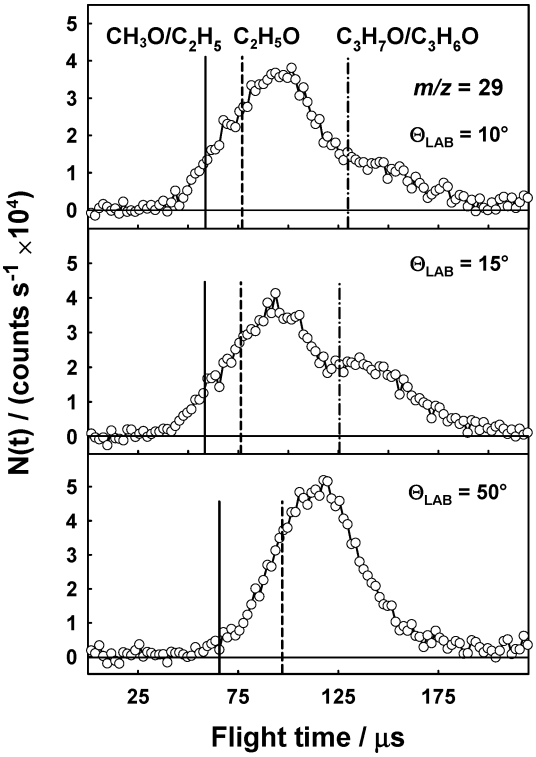

Figure 2. TOF distributions for fragments detected at $m/z = 29$ in the reaction, $O(^3P) + C_3H_8$, collected with the three detector angles shown. The solid, dashed, and dash−dot−dashed lines represent the minimum expected flight times for the products, CH_3O/C_2H_5, C_2H_5O, and C_3H_7O/C_3H_6O, respectively.

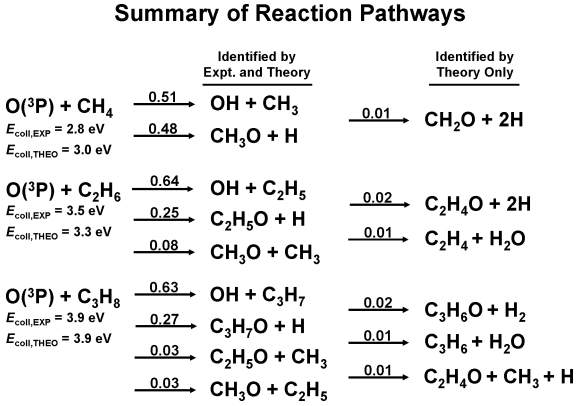

Figure 3. Summary of experimentally and theoretically observed reaction pathways for the reactions of $O(^3P)$ with methane, ethane, and propane. Theoretical relative cross sections (branching fractions) based on the MSINDO calculations are indicated as numbers over the reaction arrows.

to arise mostly from C_3H_7O products that crack to $m/z = 29$ in the ionizer. (The C_3H_7O products may also crack to give the slow signals seen in the $m/z = 30$ and 31 TOF distributions.) The faster signal is not resolved into two components, but at least some of it arrives too fast to be the result of a C_2H_5O product, indicating a reaction that leads to $CH_3O + C_2H_5$. In all of the reactions studied, products with the empirical formula, CH_3O, might represent a mixture of CH_3O and CH_2OH, as theory indicates that the initial CH_3O is produced with sufficient internal energy for rapid isomerization despite the 1.3 eV barrier.[16] Considering the large time range of the faster signal detected at $m/z = 29$ and its peak flight time, which is greater than the minimum flight time for the C_2H_5O product, it is likely that both CH_3O/C_2H_5 and C_2H_5O products are contributing to the signal at this mass-to-charge ratio. Further evidence for the production of C_2H_5O product comes from the observation of a signal at $m/z = 43$ at large detector angles (>30°), which can only be interpreted as ionizer fragmentation of C_2H_5O to the stable CH_3CO^+ ion.

Preliminary angular distributions (integrated TOF distributions as a function of laboratory angle; not shown) provide further data upon which to base inferences about the reaction mechanisms. In the c.m. frame, the OH products appear to scatter predominantly in the forward direction (i.e., the same direction as the incoming O-atoms in the c.m. frame). The C−C bond breaking channels yield CH_3O/C_2H_5 and CH_3/C_2H_5O radical fragments that scatter over a large angular range in the sideways direction with respect to the c.m. direction of the O-atom beam. The C_3H_7O (or C_3H_6O) product scatters with small c.m. velocities, making it impossible to resolve the angular (or translational energy) distribution for this product and thus draw any conclusions about its predominant scattering direction in the c.m. frame.

A summary of the reaction pathways for O + methane, ethane, and propane for which we have experimental (and theoretical) evidence is presented in Figure 3. Only empirical formulas are written for the radical products, because the velocity resolution of the data does not permit resolution of the various isomers, whose heats of formation differ relatively little.

The basic mechanisms that can be inferred from the experiments are (1) H-atom abstraction to form OH, (2) O-atom addition resulting in H-atom elimination, and (3) O-atom addition resulting in C−C bond fission. The relative yields shown in Figure 3 are based on the theoretical results that are discussed below.

V. Theoretical Results

Figure 3 contains the major (>1%) products that we have observed in our direct dynamics studies of $O(^3P) + CH_4$, C_2H_6, and C_3H_8 at the experimental energies, including MSINDO values of the branching fractions. (The B3LYP products and branching fractions agree within statistical uncertainty.) These results indicate products that can be inferred from the experimental measurements presented above and that are not observed at low collision energies. In the reaction involving methane, substantial reactivity to $OCH_3 + H$ is observed, such that the cross section for this product is comparable to that for $OH + CH_3$ at a c.m. collision energy, E_{coll}, of 3.0 eV. Other products such as formaldehyde plus two hydrogen atoms ($CH_2O + 2H$) are also seen in the calculations, although to a much lower extent. In the reaction with ethane, ethoxy radicals ($C_2H_5O + H$) are abundantly generated, although the cross section for this process at $E_{coll} = 3.3$ eV is smaller than that for abstraction ($OH + C_2H_5$). C−C breakage to give $OCH_3 + CH_3$ is also substantial, confirming the earlier predictions, based on ab initio calculations, of the barrier for this process.[7] Note, however, that the predicted relative yield for this product is well below that for ethoxy radical formation. Minority products include acetaldehyde ($C_2H_4O + 2H$), as well as water with a hydrocarbon diradical as coproduct ($H_2O + C_2H_4$). For $O(^3P) + C_3H_8$ at $E_{coll} = 3.9$ eV, the abstraction product ($OH + C_3H_7$) is the most favorable one, but products involving the formation of a C−O bond are still observed with significant probability. Among the latter products, propoxy radicals ($C_3H_7O + H$) are the most probable, followed by $CH_3O + C_2H_5$ and $C_2H_5O + CH_3$, both of which involve C−C breakage. In addition, there are several minority products that are analogous to those encountered in $O + C_2H_6$, including propanone or propanal formation plus two hydrogen atoms and water plus diradical C_3H_6.

The trajectory calculations also allow us to examine details of the microscopic reaction mechanisms. There is a clear difference between H-atom abstraction to give OH and the other reaction pathways. Abstraction to give OH closely approximates a stripping mechanism, as would be expected by analogy with other direct gas-phase reactions.[17] Thus, there is preference for high impact parameters, where the angular distributions are predominantly forward scattered (in agreement with experiments), and most of the available energy goes into relative translation. Generation of alkoxy products through H-atom elimination proceeds through smaller impact parameters, as is required for an oxygen atom to interact directly with a carbon atom. Near the saddle point, the O−C−H′ geometry (H′ being the H atom that exits) can be either collinear or bent by approximately 100°, corresponding to two different saddle points. The angular distributions that stem from these reaction paths are strongly overlapped for the translational energy considered here, as a result of the similar height of reaction barriers and the large cone of acceptance for both processes. As a result, the angular distributions are nearly isotropic. The kinematics of this product channel dictate that most of the available energy is channeled into the internal energy of the oxy product. Small impact parameters are also involved in reaction paths that give rise to C−C bond breakage. The scattering is mostly sideways, indicating saddle points having a bent O−C−C′ angle (C−C′ being the bond that breaks). As with H-atom exchange, there are two saddle points for C−C breakage, but because the experimental collision energy is much larger than the reaction barrier, the distributions are quite broad. Energy is primarily released as translation, and the energy that goes into internal energy of the fragment that bears the oxygen atom is larger than that in the coproduct.

Comparison of the present $O(^3P)$ results with earlier beam studies of low energy $O(^1D)$ reactions with alkanes[4−6] allows us to examine the possible role of intersystem crossing in the hyperthermal reactions of $O(^3P)$. For $O(^1D)$ + methane,[4] it was found that the dominant reaction was H abstraction (77%), followed by H elimination (18%), and then H_2CO formation (5%). These results show more abstraction and less elimination than the theoretical results shown in Figure 3, but our experimental branching fractions are currently not quantified enough to be distinguished from the singlet results. More dramatic differences between singlet and triplet results are found for ethane[5] and propane,[6] where C−C bond breakage dominates over abstraction or H elimination in the singlet results but not in our triplet (theory) results shown in Figure 3. The experimental product yields are again currently too poorly quantified to make a clear conclusion; however, there is evidence for enhanced C−C bond breakage compared to what theory predicts, which could be taken as evidence for singlet participation. On the other hand, the angular distribution for C−C breakage is found to have forward/backward peaks in the singlet measurements, whereas our experimental results clearly show sideways scattering of C−C bond breakage products. Although intersystem crossing effects in the reaction of $O(^3P)$ with CH_3I are known to be important,[18] theory has demonstrated a minor role[19] for the more closely related reaction, $O(^3P) + H_2$, and a recent theory/experiment comparison[12] that ignored intersystem crossing was quite good. Nevertheless, the importance of singlet states in these hyperthermal reactions remains unclear.

VI. Conclusion

New experiments on the model hyperthermal reactions of $O(^3P)$ atoms with CH_4, CH_3CH_3, and $CH_3CH_2CH_3$ show evidence for direct interaction between oxygen and carbon atoms, in addition to the H-atom abstraction channel to produce OH. The reaction $O(^3P) + CH_4$ yields signals at mass-to-charge ratios, m/z, of 29, 30, and 31 suggesting an addition reaction, $CH_3O + H$, which is confirmed by trajectory calculations. Atomic-oxygen reactions with CH_3CH_3 and $CH_3CH_2CH_3$ yield signals at $m/z = 29$, 30, 31, 43, 56 (propane only), and 57 (propane only), which again implies the production of radical fragments that contain carbon and oxygen. Various reaction pathways have been identified in the experiments with ethane and propane: $CH_3O + CH_3$, $C_2H_5O + H$, $C_2H_5 + CH_3O$, $CH_3 + C_2H_5O$, and $C_3H_7O + H$. The pathways other than H-atom abstraction have not been observed previously in the reaction of ground-state $O(^3P)$ with small alkanes. Although near-thermal reactions of $O(^3P)$ atoms with gaseous alkanes are known to produce exclusively OH, the analogous hyperthermal reactions apparently proceed often (depending on the initial translational energy and the target hydrocarbon) through addition reactions to give C−C bond fission or H-atom elimination. Theory predicts that the H-atom abstraction and O-atom addition channels have comparable probabilities. In addition, oxy radical formation is predicted to be more important than C−C bond breakage, which is a result that was not anticipated in earlier studies.[7]

Because the newly identified reactions have high barriers, they likely become important only when center-of-mass collision energies exceed ∼2 eV. Center-of-mass collision energies of gas−surface and gas-phase O-atom reactions associated with spacecraft in low-Earth orbit do exceed 2 eV; therefore, the mechanisms that have been inferred from this new work probably play a significant role in the O-atom-induced degradation of hydrocarbon materials on spacecraft and in the reactions of hydrocarbons in thruster exhaust plumes with atomic oxygen in the orbital environment.

Acknowledgment. This work has been supported by grants from the Department of Defense Experimental Program for the Stimulation of Competitive Research (DEPSCoR), administered by the Air Force Office of Scientific Research (Grant No. F49620-01-1-0276) and from the Air Force Office of Scientific Research through a Multiple University Research Initiative (Grant No. F49620-01-1-0335). D.J.G. gratefully acknowledges a fellowship from the Montana Space Grant Consortium. We thank M. Tagawa, H. Kinoshita, M. Dorrington, and J. Manso for assistance in data collection.

References and Notes

(1) Murad, E. *J. Spacecr. Rockets* **1996**, *33*, 131.

(2) Minton, T. K.; Garton, D. J. Dynamics of Atomic-Oxygen-Induced Polymer Degradation in Low Earth Orbit. In *Advanced Series in Physical Chemistry: Chemical Dynamics in Extreme Environments*; Dressler, R. A., Ed.; World Scientific: Singapore, 2001; pp 420−489.

(3) Ausfelder, F.; McKendrick, K. G. *Prog. React. Kinet. Mech.* **2000**, *25*, 299.

(4) Lin, J. J.; Shu, J.; Lee, Y. T.; Yang, X. *J. Chem. Phys.* **2000**, *113*, 5287.

(5) Shu, J.; Lin, J. J.; Lee, Y. T.; Yang, X. *J. Chem. Phys.* **2001**, *115*, 849.

(6) Shu, J.; Lin, J. J.; Lee, Y. T.; Yang, X. *J. Am. Chem. Soc.* **2001**, *123*, 322.

(7) Gindulyte, A.; Massa, L.; Banks, B. A.; Rutledge, S. K. *J. Phys. Chem. A* **2000**, *104*, 9976.

(8) Minton, T. K.; Zhang, J.; Garton, D. J.; Seale, J. W. *High Perform. Polym.* **2000**, *12*, 27. Zhang, J.; Minton, T. K. *High Perform. Polym.* **2001**, *13*, S467.

(9) Zhang, J.; Garton, D. J.; Minton, T. K. *J. Chem. Phys.* **2002**, *117*, 6239.

(10) Lee, Y. T.; McDonald, J. D.; LeBreton, P. R.; Herschbach, D. R. *Rev. Sci. Instrum.* **1969**, *40*, 1402. O'Loughlin, M. J.; Reid, B. P.; Sparks, R. K. *J. Chem. Phys.* **1985**, *83*, 5647.

(11) Caledonia, G. E.; Krech, R. H.; Green, D. B. *AIAA J.* **1987**, *25*, 59.

(12) Garton, D. J.; Minton, T. K.; Maiti, B.; Troya, D.; Schatz, G. C. *J. Chem. Phys.* **2003**, *118*, 1585.

(13) B3LYP/6-31G* direct dynamics calculations have been carried out using the GAMESS package of programs: Schmidt, M. W.; Baldridge, K. K.; Boatz, J. A.; Elbert, S. T.; Gordon, M. S.; Jensen, J. H.; Koseki, S.; Matsunaga, N.; Nguyen, K. A., Su, S. J.; Windus, T. L.; Dupuis, M.; Montgomery, J. A. *J. Comput. Chem.* **1993**, *14*, 1347.

(14) Ahlswede, B.; Jug, K. *J. Comput. Chem.* **1999**, *20*, 563. Jug, K.; Geudtner, G.; Homann, T. *J. Comput. Chem.* **2000**, *21*, 974. Bredow, T.; Geudtner, G.; Jug, K. *J. Comput. Chem.* **2001**, *22*, 861.

(15) Detailed results on the dynamics of $O(^3P)$ reactions with methane, ethane, and propane will be presented and discussed in future publications.

(16) Lin, J. J.; Lee, Y. T.; Yang, X. *J. Chem. Phys.* **1998**, *109*, 2975.

(17) Levine, R. D.; Bernstein, R. B. *Molecular Reaction Dynamics and Chemical Reactivity*; Oxford University Press: Oxford, UK, 1987.

(18) Alagia, M.; Balucani, N.; Cartechini, L.; Casavecchia, P.; van Beek, M.; Volpi, G. G.; Bonnet, L.; Rayez, J. C. *Faraday Discuss.* **1999**, *113*, 133.

(19) Hoffmann, M. R.; Schatz, G. C. *J. Chem. Phys*. **2000**, *113*, 9456.